Does the Arctic sea ice have a tipping point?

Michael Winton

Geophysical Fluid Dynamics Laboratory/NOAA

Submitted to *Geophysical Research Letters*

29 August 2006

Corresponding author: Dr. Michael Winton, GFDL/NOAA, P.O. Box 308, Princeton University Forrestal Campus, Princeton, NJ 08542. email: Michael.Winton@noaa.gov

Abstract

Two IPCC fourth assessment report climate models have Arctic ocean simulations that become sea-ice-free year around in 1%/year CO_2 increase to quadrupling experiments. These runs are examined for evidence of accelerated climate change associated with the removal of sea ice, particularly due to increasing surface albedo feedback. Both models become seasonally ice-free at an annual mean polar temperature of -9^{o}C without registering much impact on the surface albedo feedback or disturbing the linear relationship between Arctic Ocean climate change and that of the surrounding region. When the polar temperature rises above -5^{o}C, however, there is a sharp increase in the surface albedo feedback of one of the models, driving an abrupt elimination of Arctic ice and an increase in temperature above that expected from warming of the surrounding region. The transition to ice-free conditions is more linear in the other model, with ocean heat flux playing the primary driving role.

I. Introduction

If a glass is slowly tipped with a finger, it eventually reaches a point where its upright equilibrium becomes unstable and it proceeds rapidly to a new stable equilibrium on its side. Although climate models show that global temperature change is mainly linear in climate forcings over a broad range (Hansen et al, 2005), nonlinear or abrupt change may be more prevalent at regional scales. The nonlinear relationship between ice albedo and temperature has been shown to be a potential source for abrupt climate change in ice-covered regions. Simple diffusive energy balance models, that represent this relationship with a step function, produce an abrupt disappearance of polar ice as the global climate gradually warms (North 1984). Cooling from this ice-free state must proceed well beyond the point where the small ice cap was removed before polar ice abruptly reestablishes. The phenomenon is known as the *small ice cap instability* (SICI) as it disallows polar ice caps smaller than a certain critical size determined by heat diffusion and radiative damping parameters. Roughly, this scale is the scale below which the ice cap is incapable of determining its own climate which then becomes dominated, instead, by heat transport from surrounding regions (North 1984). For typical parameters this critical scale corresponds to about 18^o of latitude from the pole -- a region somewhere between today's minimum and maximum Arctic sea ice in area. Although a number of aspects of these simple models are subject to criticism, a similar kind of instability was found in an atmospheric GCM by Crowley et al (1994) in a study of Carboniferous period glaciation.

The Arctic sea ice cover has been in decline since the 1950s (Vinnikov et al, 1999). This decline is most pronounced in the summer (Stroeve et al 2005). Continuing at the

current rate of decrease, the Arctic will lose all of its perennial sea ice (be seasonally ice-free) in about 100 years. It is of interest to know if this decline will be linear in a steadily warming climate or if increases in the surface albedo feedback will lead to an accelerated or unstable decline as in the simple energy balance models. The goal of this paper is to look for SICI-like nonlinearities in the climate warming experiments performed with atmosphere-ocean GCMs for the IPCC fourth assessment report.

II. Experiments

We can only be sure of observing the presence or absence of SICI in a climate warming experiment if the integration proceeds to the point where Arctic sea ice is completely removed. Beyond this point there can be no further reductions in polar surface albedo and SICI cannot occur. Unfortunately, sea ice data is currently archived for only a small subset of the experiments available in the PCMDI AR4 archive. However, we can easily infer the presence or absence of sea ice by examining air temperatures in the coldest month and annual effective surface albedos (the ratio of annual surface-up to annual surface-down shortwave fluxes). If the former is at freezing temperature and the latter is at an ocean albedo (about 0.1) then we can be assured that there is little sea ice in the particular region in either summer or winter. We focus on a region chosen to encompass the coldest part of the Arctic Ocean, the "half-cap" region north of 80N between 90E and 270E. This region is referred to as the *polar* region in the rest of the paper. Seventy nine runs of four standard experiments (1%/year CO_2 increase to doubling, 1%/year CO_2 increase to quadrupling, SRES A1B and SRES A2) were examined. Of these, only two, had years with February polar region temperatures at freezing temperature and annual surface albedos below 0.15. Thus, it is quite uncommon

for a model's Arctic ocean to become sea ice-free year around in these climate change experiments. By contrast, it is common in these runs for the Arctic sea ice to disappear in September – about half of the runs had Septembers with surface albedos less than 0.15.

The two runs which lose their Arctic sea ice year around are the 1%/year CO_2 increase to quadrupling experiments of the MPI ECHAM5 and the NCAR CCSM3.0. Of the four forcing scenarios, the quadrupling experiment attains the highest forcing level, over 7 W/m^2. Both CCSM3.0 and ECHAM5 models have dynamical sea ice components resolving ice and snow layers and open water within the ice pack. The Arctic temperature and pressure simulations of 14 of the IPCC AR4 climate models were evaluated by Chapman and Walsh (2006). The ECHAM5 model was notable for having the lowest RMS errors in both fields of the group of models analyzed. The CCMS3.0 model was notable for being the only model with a significant low bias in Arctic Ocean sea level pressure. Both models had larger Arctic warming in the 21st century simulations than the model average. For the 1%/year CO_2 increase to quadrupling experiments the NCAR model is initialized with present day conditions while the MPI model uses a pre-industrial initialization. Both models are run for nearly 300 years, well past the time of quadrupling at year 140. The atmospheric CO_2 is held constant after quadrupling but temperatures are generally still rising in the models as the ocean heat uptake declines.

III. Results

The top panel of Figure 1 shows surface albedo for the polar region as a function of time for the two model experiments. The seasonal ice state is indicated by the albedos for three months: March (blue), June (green) and September (red). The annual effective

albedo (light blue) characterizes the time-mean reflective capacity of the ice pack as the ratio of annual surface-up to annual surface-down shortwave. The NCAR model loses its September sea ice near year 50, the MPI model loses it later, at about year 100. Both models have a progression of albedo reductions moving to earlier months in the sunlit season over the course of the integrations. The March sea ice is lost abruptly in the MPI model in the CO_2 stabilized period. The March decline is more gradual in the NCAR model. The variability of March albedos after the decline indicates interpentadal appearance of ice in the NCAR model but not in the MPI model.

The lower panel of Figure 1 shows the albedos as a function of polar region temperature. The albedo changes are more similar when viewed as a function of temperature rather than as a function of time but differences remain. The MPI model albedo declines are more abrupt in temperature as well as in time. Both models become seasonally ice-free (September albedo goes flat) at a polar temperature of about -9^oC. It is noteworthy that this loss of ice does not alter the nature of the decline in effective annual albedo in either model. In both models, the declines in June and effective annual albedos track each other fairly closely as might be expected from the large weighting of June in annual value.

The rapidity of the transition to annually ice-free conditions in the ECHAM5 model and the failure of subsequent variability to produce significant ice are suggestive of an unstable transition to a new equilibrium. Since the lifetime of sea ice in the Arctic (about 10 years) is short compared to the timescale of CO_2 increase (70 years for CO_2 doubling), we can view the ice as passing through a series of quasi-equilibrated states as the warming progresses. Under this interpretation the rapid transition to the annually ice-free

state in the MPI model bears some resemblance to the SICI of simple energy balance models which occurs abruptly as the solar constant is gradually raised above a threshold value.

To explore further the connection between the transition and SICI, we look at the changes in surface albedo feedback (SAF) as the transition progresses. Using the fact that the model transitions are more similar in temperature than in time (Fig. 1), we evaluate the surface albedo feedback in three temperature eras: -15°C to -10°C (perennial to annual ice transition), -10°C to -5°C (annual ice), and -5°C to 0°C (transition to ice-free). The ALL/CLR method of Winton (2005) is used to estimate the SAF. This method parameterizes the atmospheric downward transmissivity ($\tau_{\downarrow}$) and upward reflectivity ($\alpha_{\uparrow}$) and gives the surface shortwave absorption (S_B) as a function of these and the surface albedo (α_S):

$$S_B = S_{B\downarrow} - S_{B\uparrow} = S_{T\downarrow}\tau_{\downarrow}(1-\alpha_S)/(1-\alpha_S\alpha_{\uparrow}) \qquad (1)$$

where $S_{B\downarrow}$ and $S_{B\uparrow}$ are the surface-downward and surface-upward shortwave fluxes, respectively.

Using mean values of the atmospheric parameters along with the sensitivity of surface albedo to temperature, the surface albedo feedback is estimated numerically as the impact of a 1°C temperature change:

$$SAF = S_B(\overline{\tau}_{\downarrow}, \overline{\alpha}_{\uparrow}, \overline{\alpha}_S + \frac{\partial \alpha_S}{\partial T}) - S_B(\overline{\tau}_{\downarrow}, \overline{\alpha}_{\uparrow}, \overline{\alpha}_S) \qquad (2)$$

The averages are taken over data in the three temperature eras and the surface albedo-temperature sensitivity is evaluated by linearly fitting surface albedo to air temperature using data in the three temperature ranges. Although equation 2 gives an estimate for

SAF at the surface, it has also been shown to be a good approximation to the SAF at the top of the atmosphere due to the weak response of atmospheric absorption to surface albedo changes (Winton 2005).

In both models, surface albedo feedback makes an increasing contribution to the decline in sea ice as air temperatures approach freezing (Fig. 2a). In the NCAR model the increase is gradual, consistent with the arcing decrease in effective annual surface albedo (Fig. 1). In the MPI model a sharp increase occurs in the transition to ice-free temperature range, consistent with the kinked shape of the effective annual albedo decline for that model. In the MPI model, the SAF is 2.3 $W/m^2/^oC$ in the -5^oC to 0^oC temperature range. For comparison, the global total feedback of a group of models studied by Colman (2003) averaged about -1.1 $W/m^2/^oC$. According to the linear model, an increase of 1.1 $W/m^2/^oC$ in this global total feedback would lead to global climate instability. The Arctic generally warms at about twice the rate of the globe in simulations forced by increased CO_2, indicating a smaller (negative) feedback than for the globe. The formulation and diagnosis of regional feedbacks is less developed than for global and does not currently allow a determination of the increase in SAF needed to drive a local instability as in the SICI. Nevertheless, the magnitude of the SAF increase in the MPI model is large enough to, at least, significantly reduce the stability of its polar climate.

Figure 2b shows the monthly contributions to the SAF of the two models in the three temperature ranges. As the warming progresses, there is a shift to earlier months in the sunlit season. This shift allows the SAF to increase even as the ice-free season appears and grows. The early months of the sunlit season potentially contribute more to SAF than the later months for two reasons:

(1) Surface albedos are initially larger so there is the potential for a larger albedo reduction as the ice is removed exposing the low albedo seawater. Figure 1 shows that September albedos are 0.1 to 0.2 lower than those in March at the beginnings of the runs.

(2) Atmospheric transmissivities are largest in the spring and decline through the summer to a minimum in September in both models.

Ignoring multiple cloud-ground reflection, the SAF is the product of the product of the downward atmospheric transmissivity and the surface albedo change, so these two factors compound each other.

The pattern of surface albedo decline in the CCSM3.0 model (not shown) shows a plume of reduced albedo penetrating into the half-cap region from the Kara Sea, indicating an oceanic influence in the decline. This interpretation is borne out by an examination of the polar region heat budgets for the two models shown in Fig. 3. These budgets are constructed by regressing the fluxes on temperature in the three temperature ranges. The slopes are then multiplied by 5^{o}C to give a representative flux change between the beginning and end of the specified temperature era. Figure 3 shows that the large increase of SAF in the MPI model at warmer temperatures also appears in the overall shortwave budget of the region and there is a smaller increase in the shortwave budget of the NCAR model. The outgoing longwave radiation has a small damping effect on the warming of the region in both models. The surface budget changes are quite different: the MPI model has only small changes while the NCAR model has a large increase in surface forcing as the ocean supplies increased heating. This ocean heating contributes more to the warming of the NCAR model in the warmest temperature era than the SAF. The atmospheric heat transport convergence shifts from a forcing for the

warming in the coldest temperature era to damping the warming in the two warmer eras in both models. It is this change in atmospheric convergence of heat, rather than the OLR, that does the most to balance the forcing factors: shortwave in MPI, shortwave plus surface in NCAR. All of the surface flux changes are opposite to the atmosphere flux convergences in their impacts on the warming. The sum of the atmospheric convergence and surface flux changes (the net top-of-atmosphere flux, not shown) follows the atmospheric convergence change in sign in both models. Thus the changes in atmospheric fluxes, oceanic fluxes, and their sum all switch between forcing and damping the warming as the warming progresses. Since the polar region systematically warms more than the surrounding regions (Fig. 4), these flux changes are also alternating between up and down the temperature change gradient. Hence the down-gradient diffusive parameterization of heat transports in the energy balance models is an inadequate representation of the complex transport changes occurring in the AOGCMs.

The ratio of polar temperature change to that of the broader Arctic (60N-90N) gives an indication of the climate impact of the transition to ice-free conditions. Fig. 4 shows the relationship between polar and Arctic temperatures (top) and Arctic and global temperatures (bottom) for the two models over the course of the 1%/year to 4X CO_2 runs. The warmest polar temperature attained in the two models is about the same but the global temperature rise is considerably larger in the MPI model, while the Arctic/global and polar/Arctic amplifications are correspondingly smaller. The lines in Fig. 4 are fits to the relationships for data with polar temperatures less than -5^{o}C. A deviation from this fit at warmer temperatures might reflect the enhanced warming due to the dramatic changes in sea ice cover above this temperature in both models. The relationship is mainly linear

in both models but in the ECHAM5 model the polar temperature rises above the reference line starting at a polar temperature of -4^{o}C until it is about 2^{o}C larger and then begins to parallel the fitted line at a polar temperature of 0^{o}C. Apparently the large increase in surface albedo feedback in this range of temperatures (discussed above) plays a role in this extra warming of the polar region. After the ice is eliminated, the SAF drops to zero, and further warming falls below the -4^{o}C to 0^{o}C ratio. The behavior of the CCSM3.0 is somewhat different. At -5^{o}C the polar temperature rises slightly above the fitted line but then parallels it as both regions warm further. In both cases, the transition to seasonally ice free at a polar temperature of -9^{o}C does not disturb the linear relationship between warming in the two regions. The relationship between Arctic and global temperatures (Fig. 4, bottom) is quite linear in both models indicating that the nonlinear changes in the Arctic ocean do not have significant impacts on the broader region temperatures. Although the elimination of Arctic sea ice would doubtless have enormous consequences for the local environment, these models do not show it to be particularly important for the larger scale climate changes.

IV. Summary

Of a large number of IPCC AR4 climate model runs examined, only two warm to the point of year-around elimination of Arctic sea ice. This study has focused on the potential for this transition to have nonlinear impacts on the progress of climate change, particularly due to changes in the surface albedo feedback. Below a polar temperature of -5^{o}C there is no indication of nonlinearity in either model. Above this temperature, one of the model's (MPI) undergoes an accelerating, then decelerating, polar climate change that is associated with increased surface albedo feedback. The MPI model behavior is

similar to the small ice cap instability of simple energy balance models in that a large increase in surface albedo feedback leads to an abrupt loss of a substantially sized ice cover. The lack of interpentadal appearance of ice after this transition favors the interpretation of the post-transition state as a new stable equilibrium. The NCAR model has a smaller enhancement of climate change above -5^{o}C associated with a combination of increased surface albedo feedback and ocean heat flux. Some ice appears interpentadally after the transition. Thus, the model results are equivocal on the mechanism and magnitude of enhanced climate change associated with the removal of Arctic sea ice but are in agreement that it is a process that occurs only after considerable warming (about 13^{o}C above modern) and is geographically confined.

Acknowledgments: The author thanks Dirk Notz, Isaac Held and Ron Stouffer for helpful comments on the manuscript. The author also acknowledges the international modeling groups for providing their data for analysis, the Program for Climate Model Diagnosis and Intercomparison (PCMDI) for collecting and archiving the model data, the JSC/CLIVAR Working Group on Coupled Modeling (WGCM) and their Coupled Model Intercomparison Project (CMIP) and Climate Simulation Panel for organizing the model data analysis activity, and the IPCC WG1 TSU for technical support. The IPCC Data Archive at Lawrence Livermore National Laboratory is supported by the Office of Science, U.S. Department of Energy.

References

Chapman, W.L., and J.E. Walsh, 2006: Simulations of Arctic temperature and pressure by global climate models, submitted to *J. Climate*.

Colman, R., 2003: A comparison of climate feedbacks in general circulation models, *Climate Dynamics*, **20**, 865—873.

Crowley, T.J, K-J Yip, and S.K. Baum, 1994: Snowline instability in a general circulation model: Application to Carboniferous glaciation, *Climate Dynamics*, **10**, 363—376.

Hanson, J., and 45 coauthors, 2005: Efficacy of climate forcings, *J. Geophys. Res*, **110**, D18104, doi:10.1029/2005JD005776.

North, G.R., 1984: The small ice cap instability in diffusive climate models, *Journal of Atmospheric Sciences*, **41**, 3390—3395.

Stroeve, J., M.C. Serreze, F. Fetterer, T. Arbetter, W. Meier, J. Maslanik, K. Knowles, 2005: Tracking the Arctic's shrinking ice cover; another extreme September sea ice minimum in 2004, *Geophys. Res. Lett.*, **32**, L04501, doi:10.1029/2004GLO21810.

Vinnikov, K.Y., A. Robock, R.J. Stouffer, J.E. Walsh, C.L. Parkinson, D.J. Cavalieri, J.F.B. Mitchell, D. Garrett, and V.F. Zakharov, 1999: Global warming and Northern Hemisphere sea ice extent, *Science*, **286(5446)**, 1934—1937.

Winton, M., 2005: Simple optical models for diagnosing surface-atmosphere shortwave interactions, *J. Climate*, **18**, 3796—3805.

Winton, M., 2006: Amplified Arctic climate change: What does surface albedo feedback have to do with it? *Geophys. Res. Lett.*, **33**, L03701, doi:10.1029/2005GL025244.

Captions

Figure 1: Polar region albedo as a function of time (top) and annual mean polar region surface temperature (bottom) for the MPI ECHAM5 (circles) and NCAR CCSM3.0 (plusses) models. All data have been 5-year boxcar filtered.

Figure 2: Polar surface albedo feedback in three temperature eras (top). Monthly contributuion to polar surface albedo feedback (bottom) for surface temperatures less than -5C (dashed) and between -5 and 0C (solid) for the NCAR CCSM3.0 (black) and MPI ECHAM5 (gray) models. All data have been 5-year boxcar filtered.

Figure 3: Polar atmosphere heat balance changes over three temperature eras.

Figure 4: Polar vs. Arctic temperature (top) and Arctic vs. global temperature (bottom) for MPI ECHAM5 (circles) and NCAR CCSM3.0 (plusses). All data have been 5-year boxcar filtered.

Figure 1: Polar region albedo as a function of time (top) and annual mean polar region surface temperature (bottom) for the MPI ECHAM5 (circles) and NCAR CCSM3.0 (plusses) models. All data have been 5-year boxcar filtered.

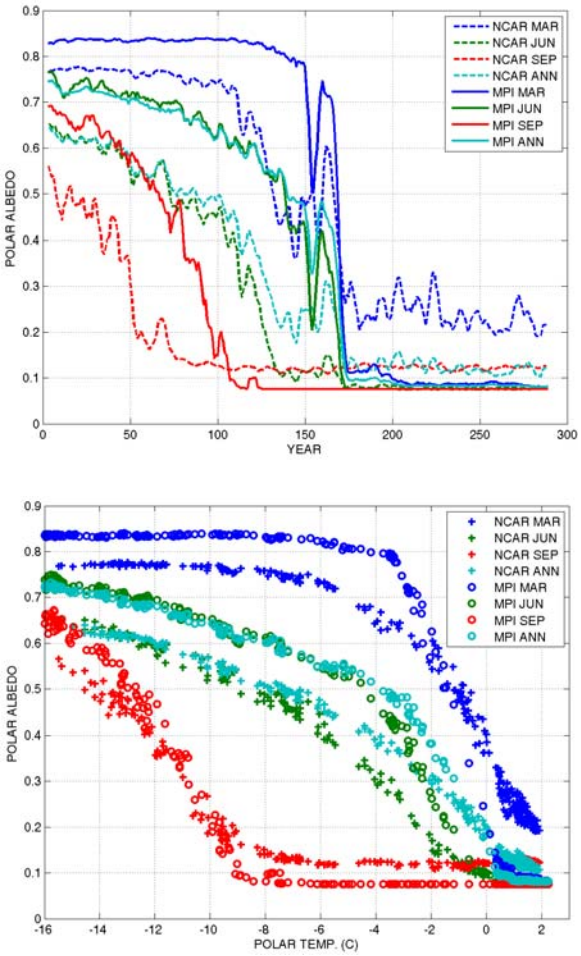

Figure 2: Polar surface albedo feedback in three temperature eras (top). Monthly contributuion to polar surface albedo feedback (bottom) for surface temperatures less than -5C (dashed) and between -5 and 0C (solid) for the NCAR CCSM3.0 (black) and MPI ECHAM5 (gray) models. All data have been 5-year boxcar filtered.

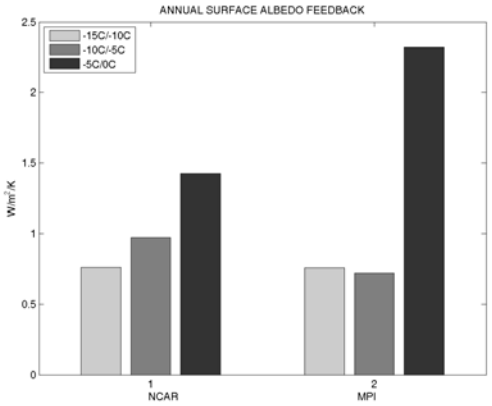

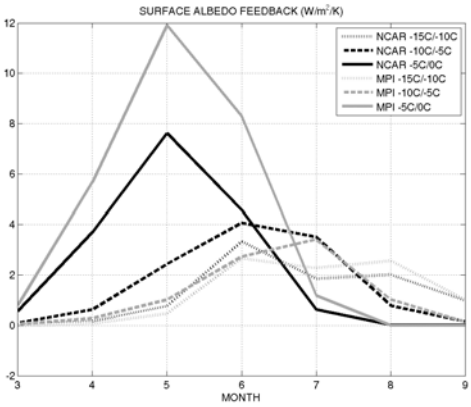

Figure 3: Polar atmosphere heat balance changes over three temperature eras.

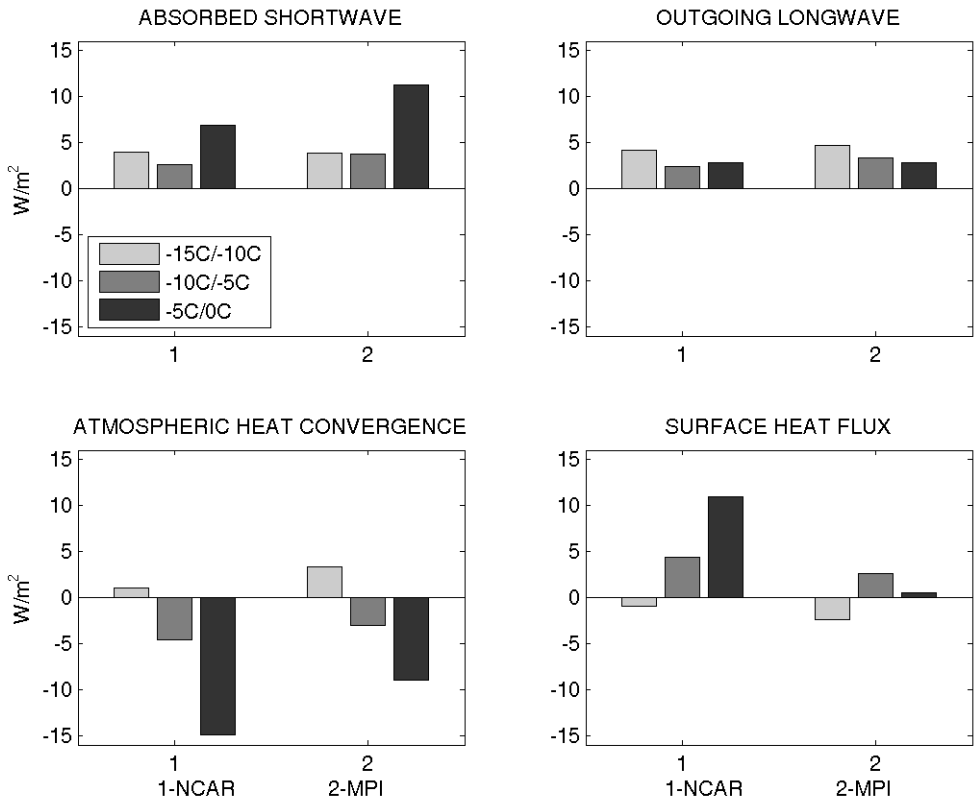

Figure 4: Polar vs. Arctic temperature (top) and Arctic vs. global temperature (bottom) for MPI ECHAM5 (circles) and NCAR CCSM3.0 (plusses). All data have been 5-year boxcar filtered.